Spatial relationship of tertiary lymphoid structures and PMN-MDSCs in bladder cancer and prognostic potential for PD-L1 immunotherapy

Anna Juncker-Jensen[1] · Xuechun Wang[2] · Gang Huang[2] · Xuemin Lu[2] · Liang Cheng[2] · Xin Lu[2]

NeoGenomics Laboratories[1] & The University of Notre Dame[2]

Keystone IO Cancer Therapy 2024

Background

Tertiary lymphoid structures (TLSs) are organized clusters of immune cells found in non-lymphoid tissues including solid tumors. TLSs are associated with favorable responses to immune checkpoint blockade (ICB) independent of programmed death-ligand 1 (PD-L1) status. TLSs may also contain immunosuppressive cells such as regulatory T cells and polymorphonuclear myeloid-derived suppressor cells (PMN-MDSCs) that suppress effector T cells. The relative distribution of TLSs and PMN-MDSCs has not been studied in human cancers.

Methods

We designed a study to investigate the distribution of immune cells inside and near the TLSs of bladder cancer and to evaluate the prognostic significance of TLSs and PMN-MDSCs in bladder cancer patients treated with ICB therapy. We performed a retrospective study using FFPE samples from 26 primary bladder cancers. Samples were stained with H&E to recognize 58 TLS regions of interest (ROIs), which were further stained with a 14-marker panel using MultiOmyx™ multiplexed IF technology.

Results

58 TLSs were classified into 23 early TLSs (E-TLSs) and 35 follicle-like TLSs (FL-TLSs) based on the morphology. To examine the spatial distribution of immune cells relative to TLSs, we set the TLS-ROIs as the center and selected ROIs 500 μm and 1,000 μm away as near-TLS-ROIs and far-TLS-ROIs. Lymphocytes were most abundant in the TLS-ROIs and decreased as the distance from TLSs increased and similar patterns were observed for PMN-MDSCs. Next, we assessed the clinical association between TLSs and PMN-MDSCs using gene signatures based on the IMvigor210 phase 2 trial of atezolizumab (anti-PD-L1) on advanced urothelial carcinoma and we found TLS signatures to be associated with better survival. When patients were stratified based on TLS and PMN-MDSC signatures, the survival from favorable to unfavorable followed the order TLS^{high}PMN-MDSC^{low} > TLS^{high}PMN-MDSC^{high} > TLS^{low}PMN-MDSC^{low} > TLS^{low}PMN-MDSC^{high}.

Table 1. Patient demographics

Parameter	Value
Number of patients	26
Age (years)	
median	63.5
Range	40-81
Gender (cases)	
Male	25
Female	1
pT-status (cases)[a]	
Ta	3
T1	4
T2	11
T3	6
T4	1
Not determined	1
LN metastasis status	
Yes	5
No	21

Table 2. Co-expressions for 14-marker panel.

Co-expressions	Phenotype
CD3+CD4+	T helper
CD3+CD4+FoxP3+	T regulatory
CD3+CD8+	Cytotoxic T cell
CD3-CD20+	B cell
CD11b+HLADR+	MHC-II+ myeloid
CD11+HLADR-	MDSC
CD11+HLADR-CD14+CD15-	M-MDSC
CD11+HLADR-CD14-CD15+	G-MDSC/TAN
CD11+HLADR-CXCR2+	CXCR2+ MDSC
CD68+	TAM
CD68+HLADR+, CD68+iNOS+	M1 TAM
PNAd+	HEV
PanCK	Epithelia

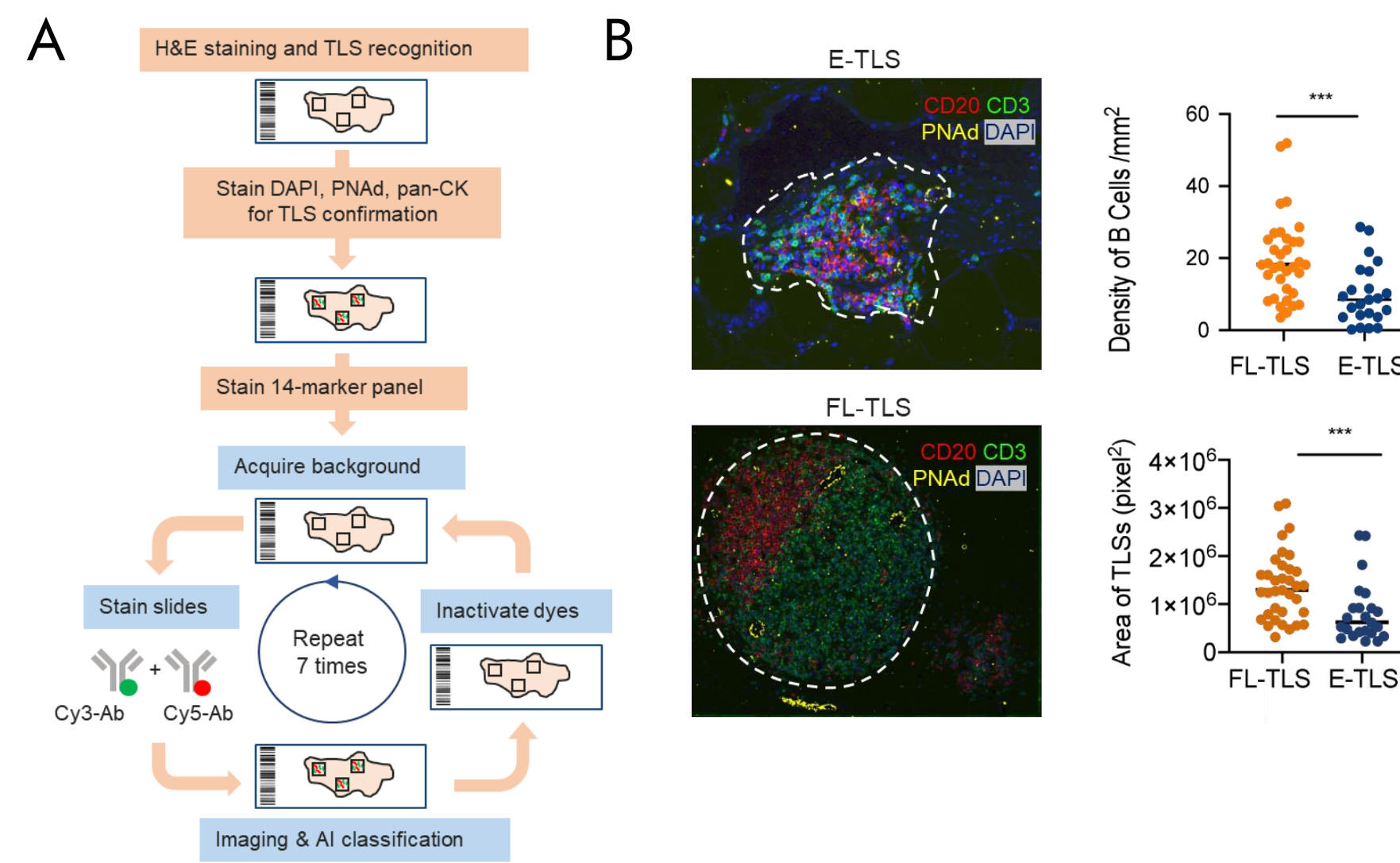## MultiOmyx Analysis of TLSs and Immune Populations

Figure 1. (A) Project workflow. Two conjugated fluorescent antibodies are applied per imaging round followed by image acquisition of the stained slides. The dye is then erased, enabling a subsequent round of staining with another pair of fluorescent antibodies. Once imaging is complete, AI algorithms segment and phenotype cells. (B) Representative images of early (E) and follicle-like (FL) TLSs. (C) Densities of B cells (upper) and TLS area sizes (lower).
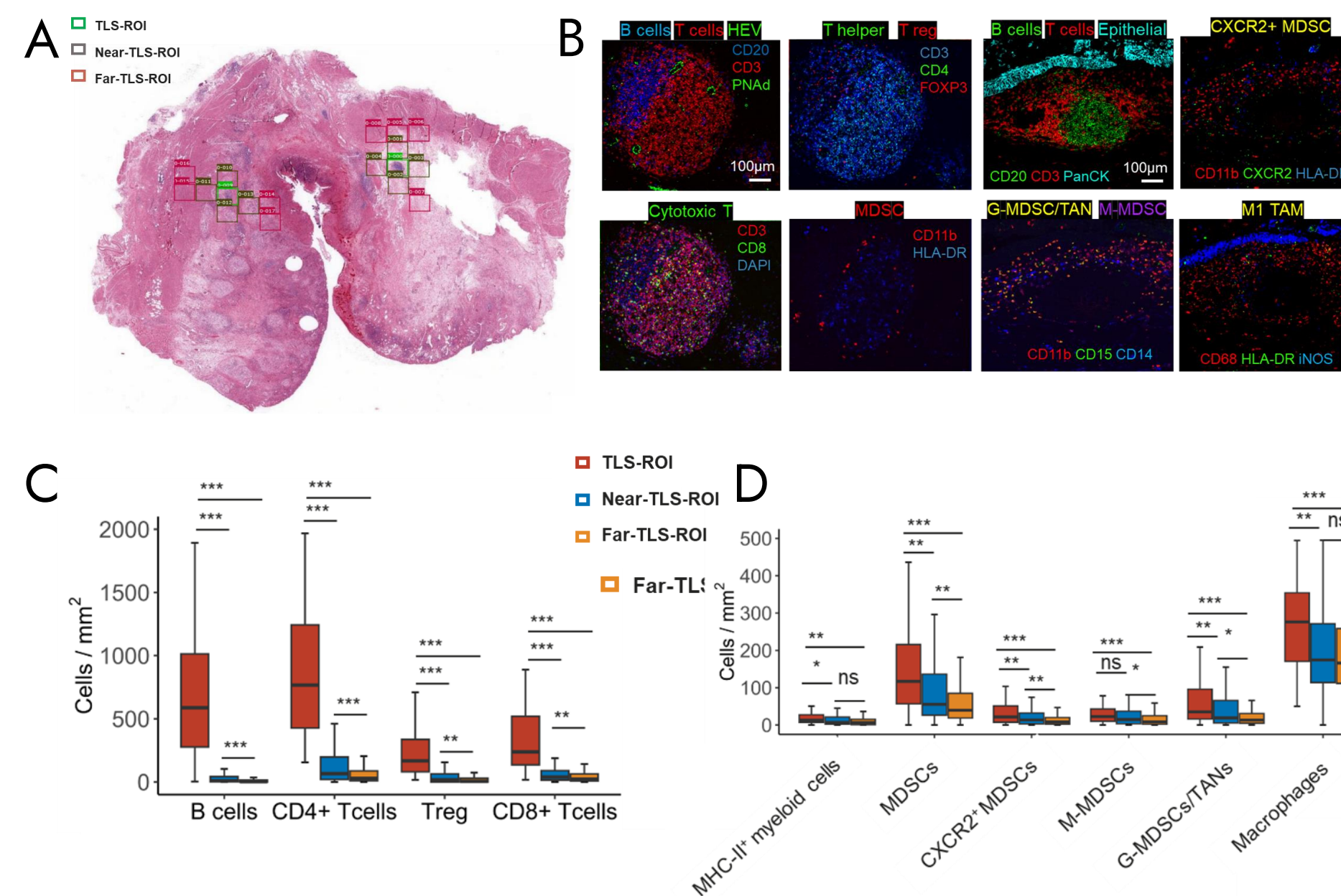

Figure 2. (A) Representative H&E marked with TLS ROIs (light green), near-TLS ROIs (dark green), and far-TLS ROIs (red). (B) Two representative follicles-like TLSs MultiOmyx IF overlay images. (C) Comparison of the densities of various lymphocytes in TLSs, near-TLSs, and far-TLSs. (D) Comparison of the densities of various myeloid cells in TLSs, near-TLSs, and far-TLSs.

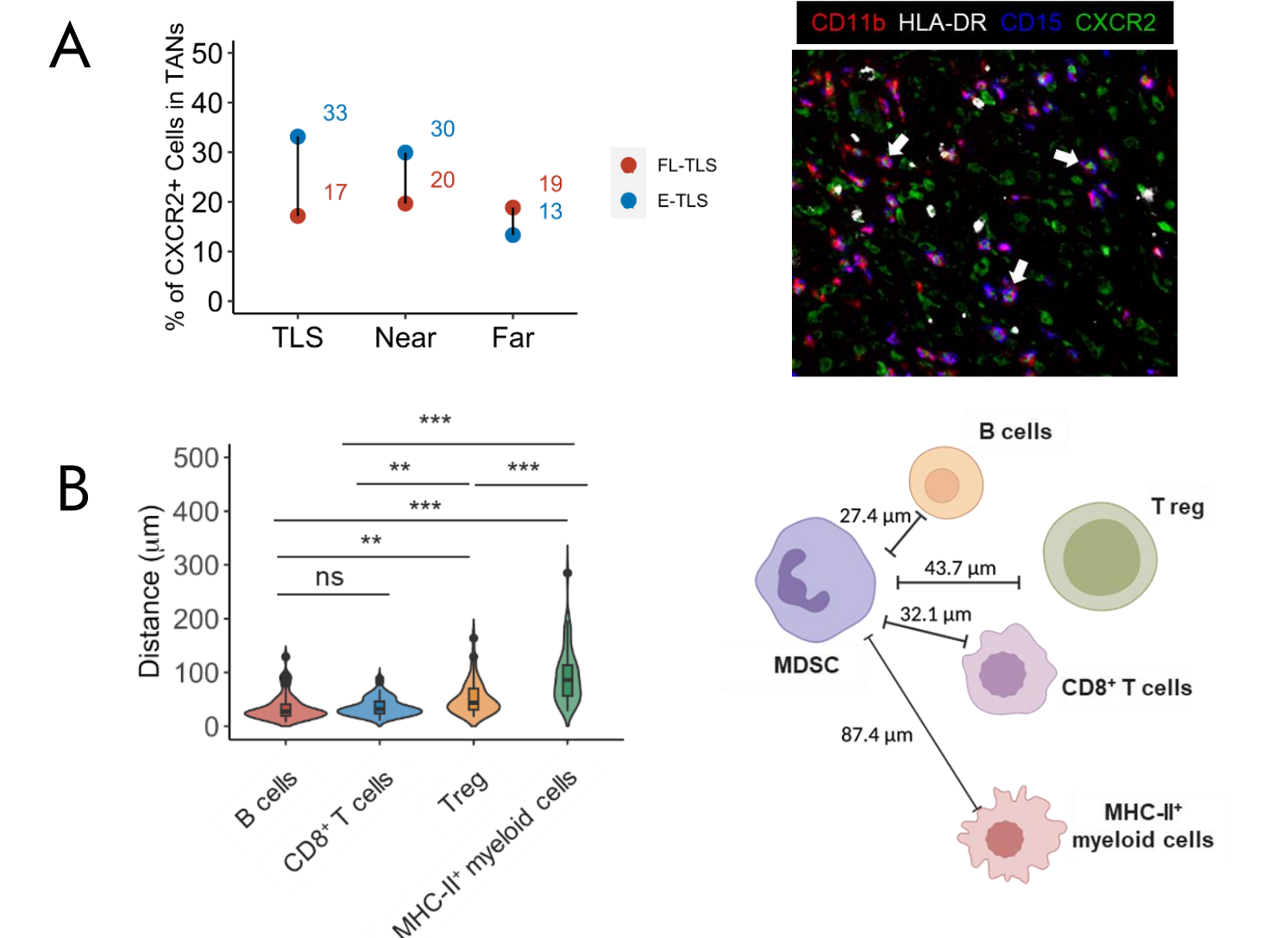## Immune Cell Subsets and Intercellular Distances

Figure 3. (A) Percentage and representative image of CXCR2+ PMN-MDSC/TANs in FL-TLS and E-TLS in 3 ROI types (TLS, near-TLS, and far-TLS). (B) Violin plots showing the distances from MDSCs to other immune cell types, and a schematic illustrating the median distances.
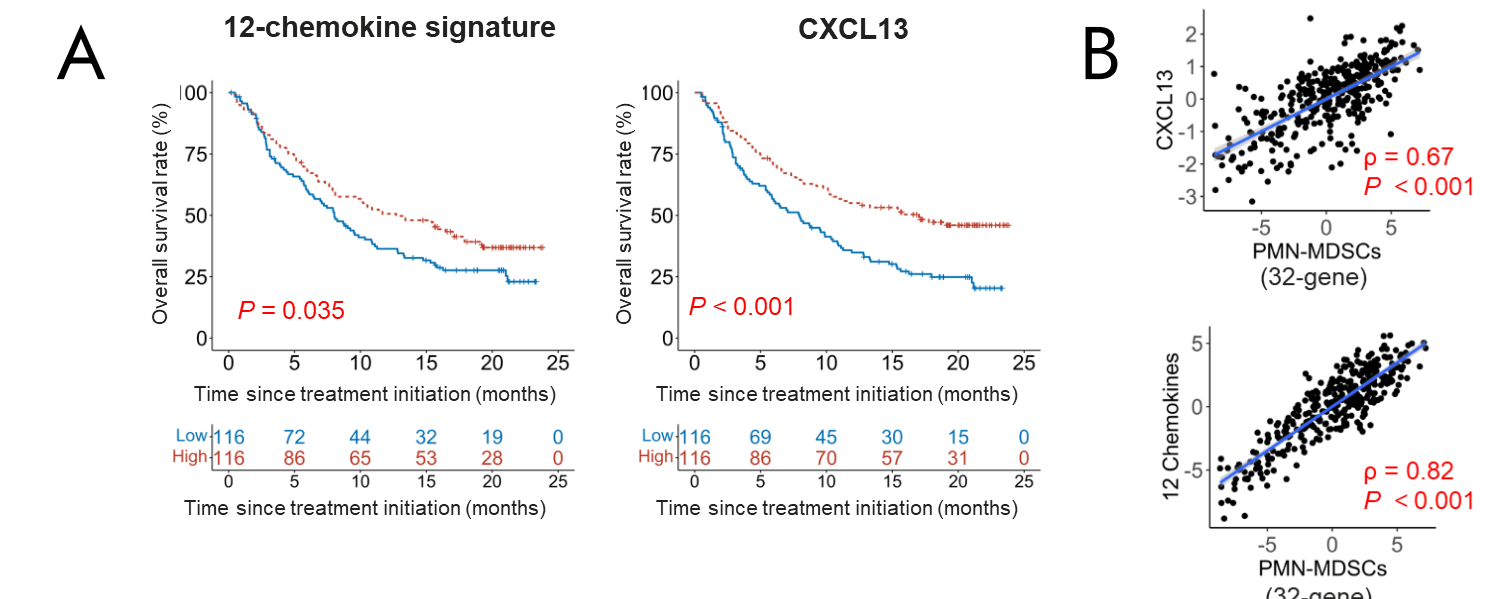
Overall Survival & Correlations

Figure 4. (A) Overall survival of the upper and lower tertiles of patients in IMvigor210 based on 12-chemokine signature or CXCL13 expression. (B) Correlation of CXCL13 gene expression or 12-chemokine signature with either of the two PMN-MDSC gene signatures based on the IMvigor210 dataset.
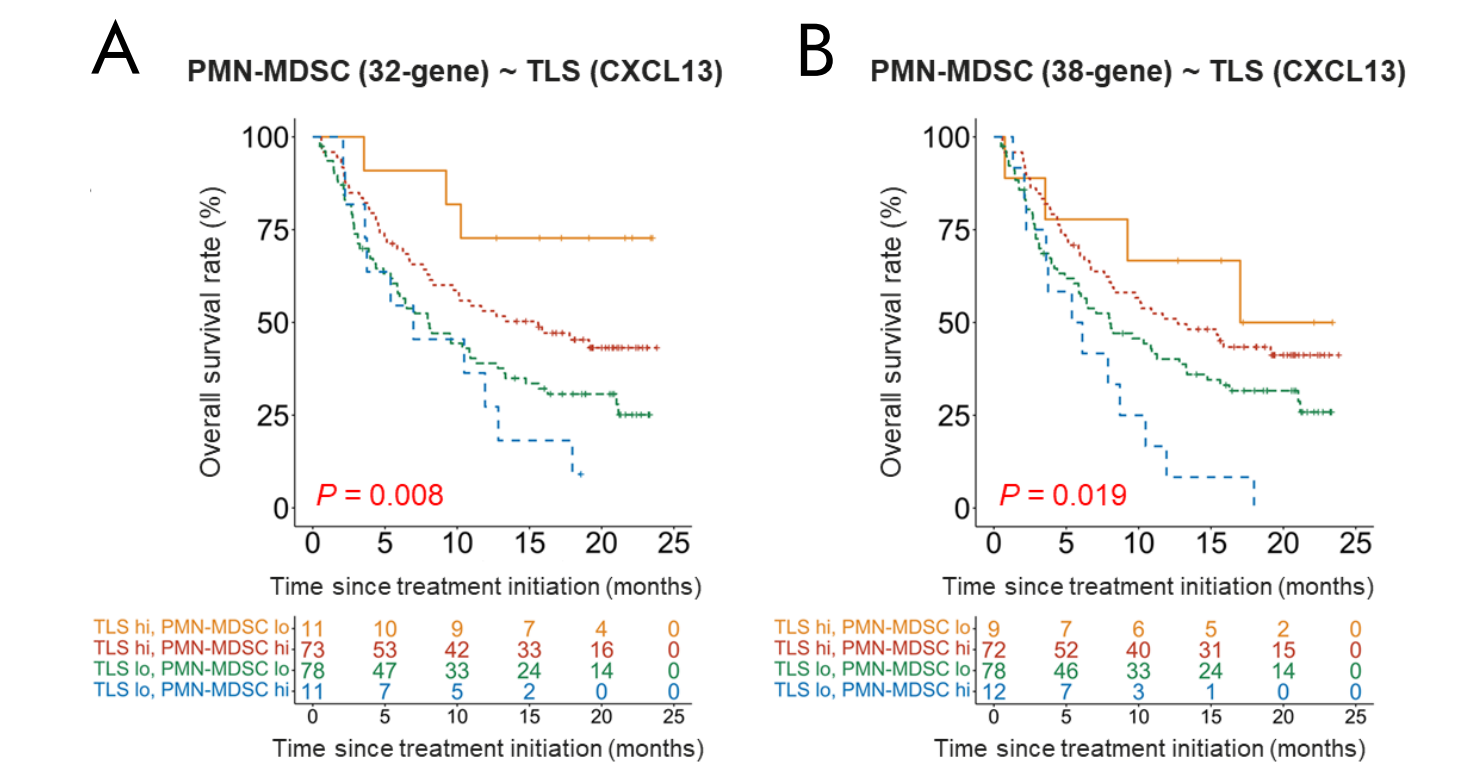
Overall Survival Analysis

Figure 5. Kaplan-Meier analysis for overall survival of patients in Imvigor210 classified into four groups based on CXCL13 expression (TLS marker) and either of two PMN-MDSC gene signatures; (A) 32-gene signature, and (B) 38-gene signature. Upper and lower tertiles were classified as high (hi) and low (lo), respectively. P values are based on two-sided log-rank tests.
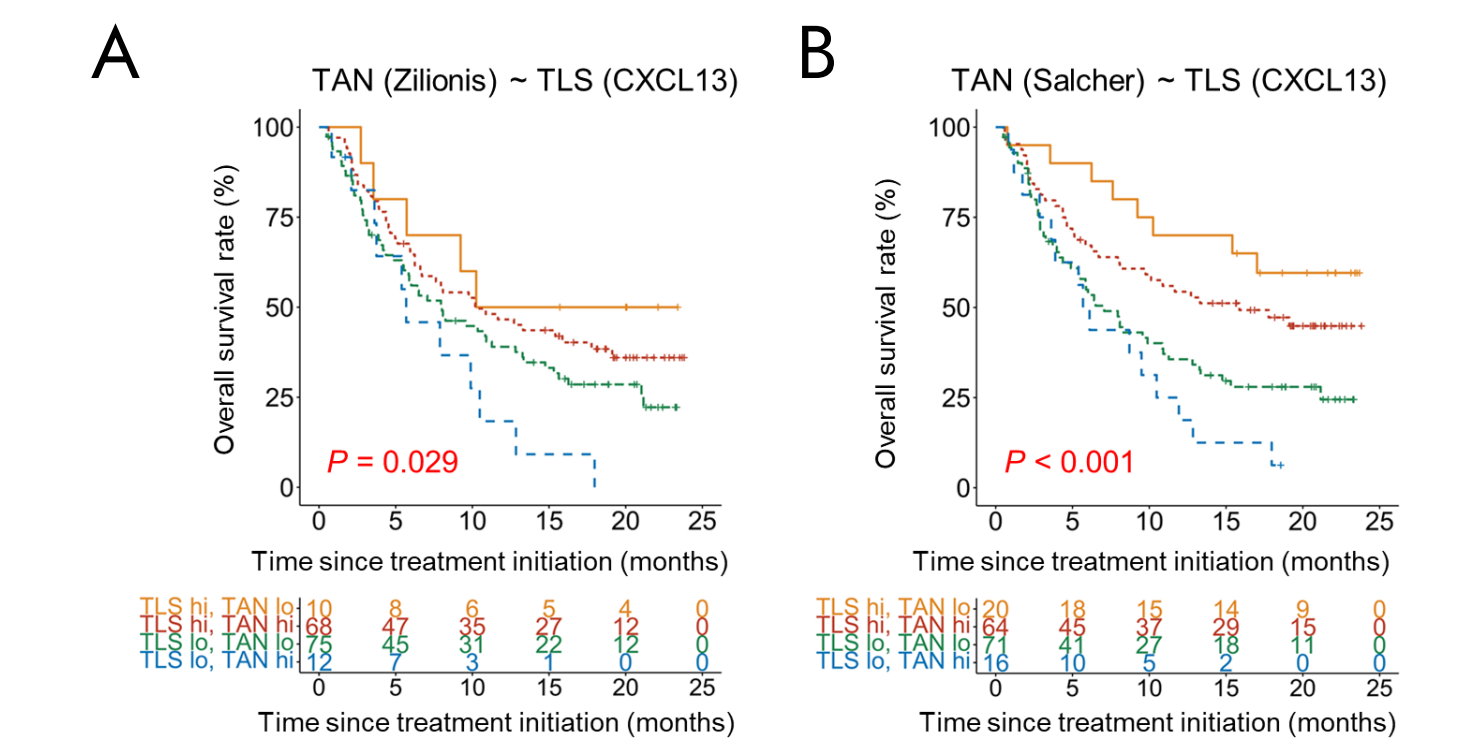

Figure 6. Kaplan-Meier analysis for overall survival of patients in Imvigor210 classified into four groups based on CXCL13 expression (TLS marker) and either of two tumor-associated neutrophil (TAN) gene signatures; Upper and lower tertiles were classified as high (hi) and low (lo), respectively. P values are based on two-sided log-rank tests.

Take-Aways

- Lymphocytes and immunosuppressive myeloid cells were most abundant in mature TLSs of bladder cancer, with densities decreasing as the distance from TLSs increased.
- Patients with bladder cancer characterized as TLS^{high}PMN-MDSC^{low} and TLS^{low}PMN-MDSC^{high} showed the best and worst prognosis with anti-PD-L1 therapy, respectively.
- These results may have the following clinical implications: (i) an immune score based on TLS^{high}PMN-MDSC^{low} may help select patients who would benefit most from ICB therapy; (ii) for TLS^{low}PMN-MDSC^{high} patients, strategies to induce TLS formation and debilitate PMN-MDSCs may help overcome ICB therapy resistance.